CMI

CORRESPONDENCE   OPEN

Check for updates

SARS-CoV-2 interaction with Siglec-1 mediates *trans*-infection by dendritic cells

Daniel Perez-Zsolt[1,16], Jordana Muñoz-Basagoiti[1,16], Jordi Rodon[2,16], Marc Elosua-Bayes[3,16], Dàlia Raïch-Regué[1], Cristina Risco[4], Martin Sachse[4], Maria Pino[5], Sanjeev Gumber[6,7], Mirko Paiardini[5,6], Jakub Chojnacki[1], Itziar Erkizia[1], Xabier Muñiz-Trabudua[1], Ester Ballana[1,8], Eva Riveira-Muñoz[1], Marc Noguera-Julian[1,11], Roger Paredes[1], Benjamin Trinité[1], Ferran Tarrés-Freixas[1], Ignacio Blanco[8], Victor Guallar[9,10], Jorge Carrillo[1], Julià Blanco[1,8,11], Amalio Telenti[12], Holger Heyn[3,13], Joaquim Segalés[14,15], Bonaventura Clotet[1,8,11], Javier Martinez-Picado[1,8,10,11,17 ✉], Júlia Vergara-Alert[2,17 ✉] and Nuria Izquierdo-Useros[1,8,17 ✉]

Antigen-presenting cells (APCs) may be resistant to SARS-CoV-2 infection but still contribute to viral pathogenesis. Lectins such as sialic acid-binding Ig-like lectin 1 (Siglec-1/CD169) mediate the attachment of viruses to APCs. Here, we show that APCs effectively capture SARS-CoV-2 within compartments via recognition of Siglec-1. This receptor interacts with sialylated gangliosides on membranes of SARS-CoV-2 variants, as previously shown for retroviruses or filoviruses [1]. Blockage of Siglec-1 on monocyte-derived dendritic cells (MDDCs) decreased SARS-CoV-2 viral transfer or *trans*-infection to bystander target cells. However, monocyte-derived macrophages (MDMs) capturing SARS-CoV-2 via Siglec-1 did not transmit infectious particles. The presence of pulmonary APCs co-expressing Siglec-1 and SARS-CoV-2 corroborated these findings in vivo.

We used the methodology described in the Supplementary Methods to dissect the contribution of Siglec-1 to SARS-CoV-2 pathogenesis. Siglec-1 expression is induced on APCs upon IFN-α or LPS exposure and increased in myeloid cells of COVID-19 patients [2]. Here, we tested whether this lectin could bind SARS-CoV-2 via recognition of sialylated gangliosides on viral membranes. APCs captured incoming SARS-CoV-2 in cellular compartments, eventually leading to viral degradation (Supplementary Fig. 1,2). Raji B cell lines transfected with different lectins (Supplementary Fig. 3A) were pulsed with SARS-CoV-2, washed and assessed by ELISA to measure cell-associated viral nucleocapsid content (Fig. 1A). While Raji cells trasnfected with wild-type Siglec-1 captured SARS-CoV-2, cells transfected with DC-SIGN, Siglec-5, Siglec-7 or devoid of these lectins did not (Fig. 1A). Viral uptake via Siglec-1 relied on the recognition of sialylated ligands, as observed with Raji cells transfected with the Siglec-1 mutant R116A, which lacks sialic acid recognition capacity and did not trap SARS-CoV-2 (Fig. 1A). Raji cells pretreated with the α-Siglec-1

monoclonal antibody (mAb) 7-239 reduced SARS-CoV-2 uptake (Supplementary Fig. 3B). SARS-CoV-2 variants were equally trapped via Siglec-1 but not by the mutated Siglec-1 R116A, indicating that sialic acid recognition is critical (Fig. 1B). Super-resolution microscopy of SARS-CoV-2 confirmed that GM1, one of the sialyllactose-containing gangliosides interacting with Siglec-1 [1], was detectable on 74% of virus particles (Fig. 1C). MDMs and MDDCs treated with IFN-α to induce Siglec-1 expression displayed higher SARS-CoV-2 uptake than nonactivated cells (Fig. 1D), and uptake was blocked by the α-Siglec-1 mAb 7-239 (Fig. 1E). These complementary approaches identified Siglec-1 as a central molecule mediating SARS-CoV-2 uptake via sialic acid recognition.

Once Siglec-1 binds to HIV-1 or Ebola viruses, receptors polarize and engulf particles within viral-containing compartments (VCCs) that are continuous with the plasma membrane and connected to the extracellular space [1]. To elucidate whether Siglec-1 also recruits SARS-CoV-2 to VCCs, we used confocal and electron microscopy and found Siglec-1-positive VCCs containing viral particles on activated MDDCs (Fig. 1F, G and Movie 1). Siglec-1 has a dual role in enhancing infectivity, either facilitating fusion on APCs, as is the case for the Ebola virus, or mediating transmission to other target cells in *trans*, as is the case for retroviruses [1]. Since SARS-CoV-2 fusion on APCs is limited (Supplementary Fig. 1B), we explored the relevance of viral *trans*-infection. Raji cells were exposed to SARS-CoV-2, washed and cocultured with targets expressing or not expressing ACE2 (Fig. 1H). Raji Siglec-1 cells cocultured with ACE2-expressing cells released higher amounts of SARS-CoV-2 than cells expressing the R116A mutant (Fig. 1H). A minimal viral amount was detected in cocultures with cells lacking ACE2, excluding SARS-CoV-2 replication on Raji cells or the release of initially trapped viruses (Fig. 1H). IFN-α-treated MDDCs cocultured

[1]IrsiCaixa AIDS Research Institute, 08916 Badalona, Spain. [2]IRTA, Centre de Recerca en Sanitat Animal (CReSA, IRTA-UAB), Campus de la UAB, 08193 Bellaterra (Cerdanyola del Vallès), Spain. [3]CNAG-CRG, Centre for Genomic Regulation (CRG, Barcelona Institute of Science and Technology (BIST), 08028 Barcelona, Spain. [4]Centro Nacional de Biotecnología, CSIC, 28049 Madrid, Spain. [5]Division of Microbiology and Immunology, Yerkes National Primate Research Center, Emory University, Atlanta, GA, USA. [6]Department of Pathology and Laboratory Medicine, School of Medicine, Emory University, Atlanta, Georgia, USA. [7]Division of Pathology, Yerkes National Primate Research Center, Emory University, Atlanta, Georgia, USA. [8]Germans Trias i Pujol Research Institute (IGTP), Can Ruti Campus, 08916 Badalona, Spain. [9]Barcelona Supercomputing Center (BSC), 08034 Barcelona, Spain. [10]Catalan Institution for Research and Advanced Studies (ICREA), 08010 Barcelona, Spain. [11]Present address: University of Vic–Central University of Catalonia (UVic-UCC), Vic 08500, Spain. [12]Present address: Department of Integrative Structural and Computational Biology, Scripps Research, La Jolla, CA 92037, USA. [13]Present address: Universitat Pompeu Fabra (UPF), Barcelona, Spain. [14]Present address: UAB, CReSA (IRTA-UAB), Campus de la UAB, 08193 Bellaterra (Cerdanyola del Vallès), Spain. [15]Present address: Departament de Sanitat i Anatomia Animals, Facultat de Veterinària, UAB, 08193 Bellaterra (Cerdanyola del Vallès), Spain. [16]These authors contributed equally: Daniel Perez-Zsolt, Jordana Muñoz-Basagoiti, Jordi Rodon, Marc Elosua-Bayes. [17]These authors jointly supervised this work: Javier Martinez-Picado, Júlia Vergara-Alert, Nuria Izquierdo-Useros. ✉email: jmpicado@irsicaixa.es; julia.vergara@irta.cat; nizquierdo@irsicaixa.es
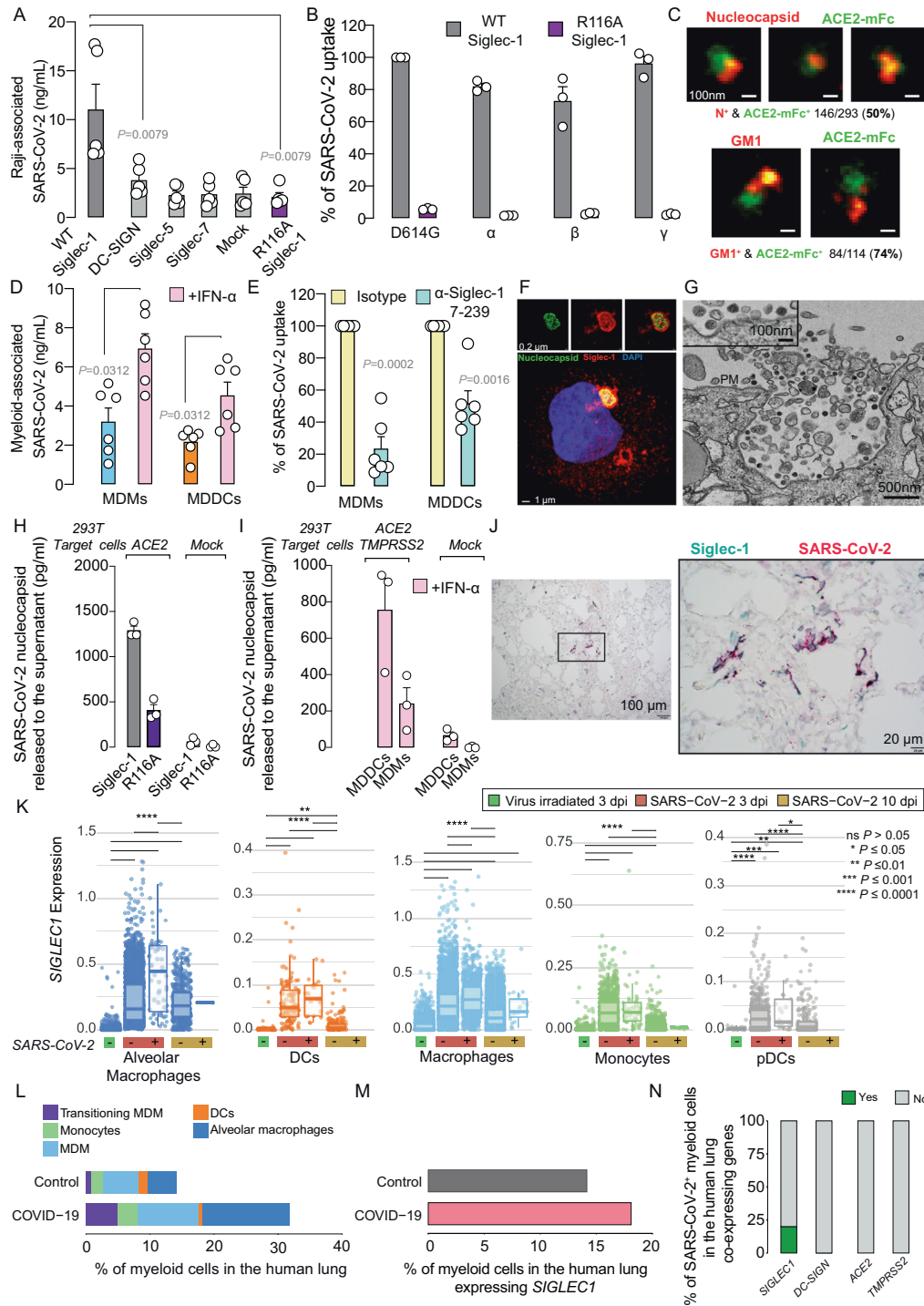
Fig. 1 SARS-CoV-2 trapped via Siglec-1 on MDDCs mediates viral *trans*-infection of target cells, and in pulmonary tissues, SARS-CoV-2 is detected on APCs expressing Siglec-1. A Uptake of SARS-CoV-2 by Raji B cells measured by ELISA from two experiments. **B** Percentage of SARS-CoV-2 variant uptake from one experiment. Values are normalized to D614G strain uptake by Siglec-1 cells, set at 100%. **C** Superresolution microscopy of SARS-CoV-2 stained with α-nucleocapsid or α-GM1 antibodies (red) and ACE2-mFc (green). The percentage of costaining is shown. **D** Uptake of SARS-CoV-2 by MDMs and MDDCs activated or not with IFN-α for 48 h from two experiments. **E** Percentage of viral uptake inhibition of IFN-α-treated APCs preincubated with mAbs from two experiments. Values are normalized to viral uptake by isotype-treated cells, set at 100%. **F, G** Confocal and electron microscopy of VCCs in LPS- and IFN-α-activated MDDCs exposed to SARS-CoV-2. See Movie 1. PM, plasma membrane. **H, I** Transmission of SARS-CoV-2 by indicated cells. APCs exposed to SARS-CoV-2 were cocultured with HEK-293T cells expressing ACE2 or not. Viral release from one experiment was measured with an ELISA. **J** Costaining with α-Siglec-1 and α-SARS-CoV-2 nucleocapsid antibodies in the lungs of an infected rhesus macaque. **K** *SIGLEC1* expression on AGM APCs containing or not containing SARS-CoV-2 RNA. Boxplots show the median, the first and third quartiles and whiskers. **L, M** Single-cell analysis of pulmonary myeloid cells of 16 COVID-19 patients and 3 controls and APCs expressing *SIGLEC1*. **N** Myeloid cells of COVID-19 patients containing viral RNA and coexpressing *SIGLEC1, DC-SIGN, ACE2* or *TMPRSS2*. **A, B, D, E, H,** and **I** show mean values and SEMs. Statistical differences were assessed with the Mann–Whitney *t* test (**A**), Wilcoxon-matched paired *t* test (**D**), one-sample *t* test (**E**), Mann–Whitney–Wilcoxon test with Bonferroni correction (**K**), scCODA (**L**), chi-square test (**M**; $P = 1.045e^{-11}$) or Bonferroni-adjusted chi-square test (**N**; $P = 0.0272624$)

with ACE2- and TMPRSS2-expressing target cells released higher amounts of SARS-CoV-2 than MDMs (Fig. 1I). Experiments with nonreplicative HIV-1 pseudotyped with SARS-CoV-2 spike confirmed Siglec-1 transmission of SARS-CoV-2 via ACE2-dependent fusion on target cells (Supplementary Fig. 4). Hence, SARS-CoV-2 retention on MDDCs via Siglec-1 allows *trans*-infection.

Lung immunohistochemistry analysis from a SARS-CoV-2-infected rhesus macaque used in a previous study [3] confirmed the codetection of Siglec-1 and viral nucleocapsid in cells with myeloid morphology (Fig. 1J). Single-cell RNA sequencing data previously collected in African green monkeys (AGMs) allowed us to focus on pulmonary APCs (Supplementary Fig. 5), where SARS-CoV-2 infection upregulated *SIGLEC1* expression 3 days post-inoculation (dpi) (Supplementary Fig. 6A). Viral RNA was detected in high numbers at 3 dpi, but the levels decreased at 10 dpi (Supplementary Fig. 6B), consistent with the resolution of infection in this mild COVID-19 model. When we compared the expression of *SIGLEC1* on APCs without or with associated viral RNA, only alveolar and interstitial macrophages containing viral RNA significantly increased *SIGLEC1* expression (Fig. 1K). Thus, infection triggers *SIGLEC1* expression on all APCs, but this phenomenon is not linked to the detection of cell-associated viral RNA. We next analyzed the most detailed single-cell atlas [4] of human lungs of COVID-19 patients with advanced disease and controls (Supplementary Fig. 7A-B). Here, APCs were enriched for viral RNA but lacked ACE2 and TMPRSS2 viral entry receptors (Supplementary Fig. 7C). Pulmonary myeloid cells were enriched in COVID-19 patients as compared to those in controls (Fig. 1L; Supplementary Fig. 8A–E), and *SIGLEC1*-expressing APCs were also enriched (Fig. 1M; Supplementary Fig. 8F). Twenty percent of pulmonary APCs expressing viral RNA also coexpressed *SIGLEC1*, whereas none coexpressed other lectins or viral receptors (Fig. 1N). These results corroborated the presence of the Siglec-1 receptor or transcripts on APCs containing SARS-CoV-2 in vivo. Targeting Siglec-1 or *trans*-infection [5] could offer cross-protection against SARS-CoV-2 and other enveloped viruses that exploit APCs for viral dissemination and lead to the development of new broad-spectrum antivirals for future outbreaks.

REFERENCES

1. Perez-Zsolt D, Martinez-Picado J, Izquierdo-Useros N. When dendritic cells go viral: the role of siglec-1 in host defense and dissemination of enveloped viruses. Viruses. 2019;12:8.
2. Bedin A-S, Makinson A, Picot MC, Mennechet F, Malergue F, Pisoni A, et al. Monocyte CD169 expression as a biomarker in the early diagnosis of coronavirus disease 2019. J Infect Dis. 2021;223:562–7.
3. Hoang TN, Pino M, Boddapati AK, Viox EG, Starke CE, Upadhyay AA, et al. Baricitinib treatment resolves lower-airway macrophage inflammation and neutrophil recruitment in SARS-CoV-2-infected rhesus macaques. Cell. 2021;184:460–75. e21
4. Delorey TM, Ziegler C, Heimberg G, Normand R, Yang Y, Segerstolpe Å, et al. COVID-19 tissue atlases reveal SARS-CoV-2 pathology and cellular targets. Nature. 2021;595:107–13.
5. Lempp FA, Soriaga LB, Montiel-Ruiz M, Benigni F, Noack J, Park YJ, et al. Lectins enhance SARS-CoV-2 infection and influence neutralizing antibodies. Nature. 2021;598:342–7. https://doi.org/10.1038/s41586-021-03925-1

ACKNOWLEDGEMENTS

AUTHOR CONTRIBUTIONS

Conceived and designed the experiments: B.C., J.M.-P., J.V.-A., and N.I.-U. Performed experiments and provided key reagents: D.P.-Z., J.M.-B., J.R., M.E., D.R.-R., C.R., M.S., M.P., S.G., M.Pa., J.C., E.B., E.R., I.E., X.M., M.N., B.T., F.T.-F., J.B., J.S., J.V.-A., and N.I.-U. Analyzed and interpreted the data: D.P.-Z., J.M.-B., J.R., M.E., D.R.-R., C.R., M.S., M.S., M.P., S.G., J.C., E.B., E.R., I.E., X.M.-T., M.N., R.P., B.T., F.T.-F., I.B., V.G., J.C., J.B., A.T., H.H., J.S., B.C., J.M.-P., J.V.-A., and N.I.-U. Wrote the paper: D.P.-Z., J.M.-B., J.R., M.E., D.R.-R., J.V.-A., and N.I.-U.

COMPETING INTERESTS

ADDITIONAL INFORMATION